Journal of Alloys and Compounds 499 (2010) 75–79

Contents lists available at ScienceDirect

Journal of Alloys and Compounds

journal homepage: www.elsevier.com/locate/jallcom

Preparation and characterization of $Ga_{2x}In_{2(1-x)}O_3$ films deposited on ZrO_2 (1 0 0) substrates by MOCVD

Lingyi Kong, Jin Ma*, Fan Yang, Caina Luan, Zhen Zhu

School of Physics, Shandong University, Jinan, Shandong 250100, PR China

ARTICLE INFO

Article history:
Received 18 November 2009
Received in revised form 8 February 2010
Accepted 11 February 2010
Available online 18 February 2010

Keywords:
$Ga_{2x}In_{2(1-x)}O_3$ film
MOCVD
Band gap
ZrO_2 substrate

ABSTRACT

$Ga_{2x}In_{2(1-x)}O_3$ films with different gallium (Ga) content x [x = Ga/(Ga + In) atomic ratio] have been deposited on ZrO_2 (1 0 0) substrates by metalorganic chemical vapor deposition (MOCVD). The structural, electrical and optical properties of obtained films have been studied. Structure analysis revealed that the films deposited with Ga content x = 0.1, 0.3 and 0.5 were polycrystalline structures of bixbyite In_2O_3 and the samples prepared with x = 0.7 and 0.9 exhibited amorphous structures. As Ga content x increased from 0.1 to 0.9, the resistivity of the films increased from 2.20×10^{-3} to 1.90 Ω cm and the optical band gap of the films monotonously broadened from 3.72 to 4.46 eV. The average transmittance of the samples in the visible range exceeded 78%.

1. Introduction

In recent years, there has been much interest in wide band gap oxide semiconductors due to their potential applications in short wavelength light emitting devices, ultraviolet (UV) photodetectors and quantum-well devices. It should be emphasized that band gap engineering is one of the key issues for the construction of various electronic and optical devices using compound semiconductors. As a typical case of ternary compounds, $Mg_xZn_{1-x}O$ is considered to be an alloy of MgO and ZnO. The band gap of $Mg_xZn_{1-x}O$ can be tuned from 3.4 to 7.8 eV by controlling the composition of this alloy suitably [1–3].

Both In_2O_3 film and Ga_2O_3 film are good transparent n-type semiconductors with direct band gap of 3.6 [4] and 4.9 eV [5], respectively. In_2O_3 film with the bixbyite structure is a very important material which shows excellent opto-electrical properties and has been widely used in many fields such as solar cells, gas sensors, liquid crystal displays and so on [6–9]. Ga_2O_3 film with the monoclinic structure (β-Ga_2O_3) is a deep-ultraviolet transparent conductive film [10], which is considered as a promising material for a new generation of optoelectronic devices [11–14]. According to the theory of Hill [15], similar to the $Mg_xZn_{1-x}O$ semiconductor alloy, In_2O_3 could be alloyed with Ga_2O_3 to tune the band gap from 3.7 to 4.9 eV depending on the Ga content x in $Ga_{2x}In_{2(1-x)}O_3$. Once $Ga_{2x}In_{2(1-x)}O_3$ semiconductor alloy is available, band-gap engineered electro-optical devices based on this material will have a wide variety of applications.

In previous literature, some reports have been published to describe the properties of Ga–In–O material [16–23]. The phase diagram of β-Ga_2O_3/In_2O_3 solid solution system has been reported by Patzke and Binnewies [16]. Chun et al. have reported single-crystalline Ga-doped In_2O_3 nanowires synthesized by thermal evaporation [17]. Cava et al. have reported transparent conductive Sn and Ge doped $GaInO_3$ films deposited by pulsed laser deposition (PLD) [18]. The electronic structure of amorphous $InGaO_3(ZnO)_{0.5}$ thin film deposited by radiofrequency magnetron sputtering has been investigated by Cho et al. [19], as well as the electrical and optical properties of transparent conductive In–Ga–Zn–O films deposited by PLD have been investigated by Inoue et al. [20]. Oshim and Fujita have reported the optical properties of Ga_2O_3-based high Ga content $Ga_xIn_{2(1-x)}O_3$ ($0.57 \le x \le 0.96$) films deposited by molecular beam epitaxy (MBE) [21]. Further more, transparent Ga-doped In_2O_3 film has been used as ohmic contact of the GaN-based light-emitting diodes (LEDs) [22], and $GaInO_3$ film has been used as the active channel material of transparent thin-film transistors (TTFTs) [23]. However, to the best of our knowledge, no reports on the electrical properties of undoped $Ga_{2x}In_{2(1-x)}O_3$ films with $0.1 \le x \le 0.9$ have been published, especially deposited on ZrO_2 substrates by means of MOCVD. In this paper, $Ga_{2x}In_{2(1-x)}O_3$ films with different Ga content ($0.1 \le x \le 0.9$) have been deposited on ZrO_2 (1 0 0) substrates at 550 °C by MOCVD. Structural, electrical and optical properties of the films have been investigated in detail.

* Corresponding author. Tel.: +86 531 88361057; fax: +86 531 88564886.
E-mail address: kly2006@mail.sdu.edu.cn (J. Ma).

0925-8388/$ – see front matter © 2010 Elsevier B.V. All rights reserved.
doi:10.1016/j.jallcom.2010.02.092

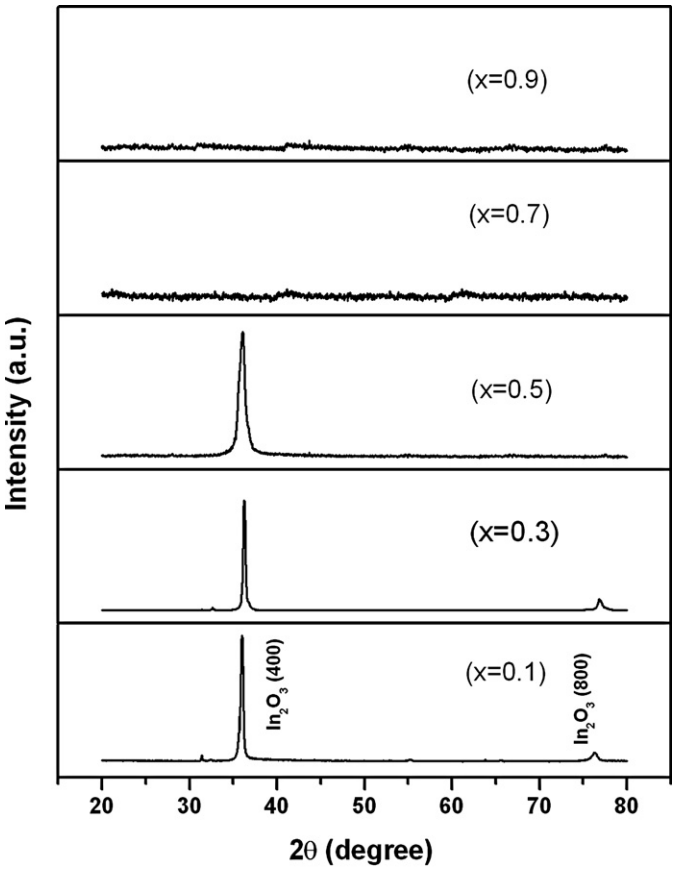

Fig. 1. XRD spectra of the $Ga_{2x}In_{2(1-x)}O_3$ films with different Ga content.

2. Experimental

The films were deposited on ZrO_2 (1 0 0) (yttrium stabilized) substrates using a high vacuum MOCVD system. Commercially available trimethylindium [$In(CH_3)_3$] and trimethylgallium [$Ga(CH_3)_3$] were used as organometallic (OM) sources. The OM sources were transported into a reactor according to the defined atomic ratio x (Ga content) by ultra high purity N_2 (9N) which was used as the carrier gas. High purity O_2 (5N) with a flow rate of 50 sccm (sccm denotes cubic centimeter per minute at STP) was injected into the reactor as the oxidant. During the deposition, the growth pressure was kept at 50 torr and the substrate temperature was kept at 550 °C.

The structural properties were determined by X-ray diffraction (XRD), in which a RIGAKU D/MAX-γB X-ray diffractometer with Cu Kα radiation was used. The scanning electron microscopy (SEM) characterization was performed with an S-4800 Ultra-high resolution scanning electron microscope. The composition of the films was determined by Rutherford backscattering spectrometry (RBS) using 2.1 MeV He^{2+} ion beam. The sheet resistivity was measured using a conventional four-probe instrument. The thickness of the films was measured by a Veeco Dektak 150 profilometer, with a measurement error about plus or minus 5 nm. The vertical resolution of the Veeco Dektak 150 profilometer is 0.1 nm, which could only be achieved in excellent measuring conditions. The Hall mobility was measured with Van der Pauw technique at room temperature. The optical transmittance spectra were determined by a Shimadzu TV-1900 double-beam UV–vis-NIR spectrophotometer in the wavelength range of 200–800 nm.

3. Results and discussion

Fig. 1 shows the XRD spectra of the $Ga_{2x}In_{2(1-x)}O_3$ films with different Ga content. The thicknesses of the films are 89, 100, 91, 119, 162 nm corresponding to $x = 0.1$, 0.3, 0.5, 0.7 and 0.9, respectively. It can be seen that, with x increasing from 0.1 to 0.5, the diffraction peaks corresponding to In_2O_3 (4 0 0) and (8 0 0) of the bixbyite structure are observed and the full width at half maximum (FWHM) of the (4 0 0) peak increases from 0.37° to 0.93°, which reveals the degradation of the crystalline quality of this alloy. As Ga content increases farther, no diffraction peak is detected from the XRD patterns. We suppose that the films with $x \geq 0.7$ have amorphous structures. It should be noted that the locations of all the measured In_2O_3 (4 0 0) diffraction peaks shift to high angle compared with the No. 06-0416 card of Joint Committee on Powder Diffraction Standards (JCPDS). The shift of the (4 0 0) peak results from that some of the In^{3+} ions in the lattice are replaced by Ga^{3+}, and the ionic radius of Ga^{3+} (0.62 Å) is smaller than In^{3+} (0.81 Å). The average crystallite size for the samples with $x = 0.1$, 0.3 and 0.5 is about 32.1, 27.8 and 12.4 nm respectively, which was calculated from the FWHM of the (4 0 0) peak using Scherrer formula [24]. For the films with $x \leq 0.5$, the prepared samples are polycrystalline films with a single orientation of In_2O_3 [1 0 0] owing to the excellent epitaxial relationship between the In_2O_3 (1 0 0) plane and the ZrO_2 (1 0 0) substrate [25]. The film with $x = 0.5$ has a bad crystalline quality, which results from the formation of the bixbyite structure became difficult as Ga content increased. For the high Ga content ($x \geq 0.7$) samples, the obtained films are amorphous which originates from that $Ga_{2x}In_{2(1-x)}O_3$ is difficult to form any detectable crystalline phase on ZrO_2 (1 0 0) substrate, especially deposited at such a lower temperature [26]. This result implies that the Ga content significantly affects the structure of the $Ga_{2x}In_{2(1-x)}O_3$ films.

The Ga content dependence of crystallinity for the $Ga_{2x}In_{2(1-x)}O_3$ films was also revealed by their SEM micrographs. The surface morphologies of the $Ga_{2x}In_{2(1-x)}O_3$ films with $x = 0.1$, 0.5 and 0.9 are displayed in Fig. 2(a)–(c), respectively. In image (a), a rough surface and large grain sizes are obviously observed. From image (b), grains with uniform and well-defined grain boundaries can also be seen. But in image (c), only a smooth surface with a few cracks and pinholes is observed, mostly because of the uncrystallized structure of the film with $x = 0.9$. The images show that, the average grain size of the films decreases and the surface becomes smooth as Ga content increases. The results imply that the films with Ga content of $x = 0.1$ and 0.5 have polycrystalline structures, and the film with high Ga content of $x = 0.9$ has an amorphous structure. The results are consistent with the XRD analyses.

Fig. 3 illustrates the RBS spectra of the $Ga_{2x}In_{2(1-x)}O_3$ films with experiment setting values $x = 0.1$, 0.5 and 0.9. The element signals of Ga and In are indicated in the spectra. The Ga contents of the $Ga_{2x}In_{2(1-x)}O_3$ films were estimated from the RBS spectra [27]. Corresponding to the above three samples, the calculated Ga contents in the films are 0.08, 0.39 and 0.80, respectively. The results show that the actual Ga contents in the films are less than the corresponding experiment setting values, which originates from that $Ga(CH_3)_3$ is less chemically active and has a lower percent conversion compared with $In(CH_3)_3$ during the oxidation process.

Fig. 4 shows the resistivity, Hall mobility and carrier concentration of the $Ga_{2x}In_{2(1-x)}O_3$ films as a function of Ga content. It reveals that, with increasing Ga content x from 0.1 to 0.9, the Hall mobility decreases from 42.40 to 1.96 $cm^2\ v^{-1}\ s^{-1}$ and the carrier concentration decreases from 6.70×10^{19} to $1.68 \times 10^{18}\ cm^{-3}$. Correspondingly, the resistivity of the films increases monotonously from 2.20×10^{-3} to 1.90 Ω cm. The decrease of Hall mobility is due to the degradation of the crystalline quality as Ga content increases. With rising Ga content, the grain size becomes smaller, as well as the increased defects in the films, leads to the corresponding scattering enhance. Since the position of conduction band bottom of Ga_2O_3 is relatively high, the donor levels tend to become deep levels [10]. Corresponding to the increasing Ga content, the band gap of the $Ga_{2x}In_{2(1-x)}O_3$ films widens gradually and introduction of shallow donor levels into the compound for efficient release of electrons into conduction band becomes more difficult. As deep levels provide less free charge carriers, the carrier concentration of the films decreases monotonously. Because of the decreased carrier concentration and decreased Hall mobility, the resistivity of the films increases monotonously as Ga content increases.

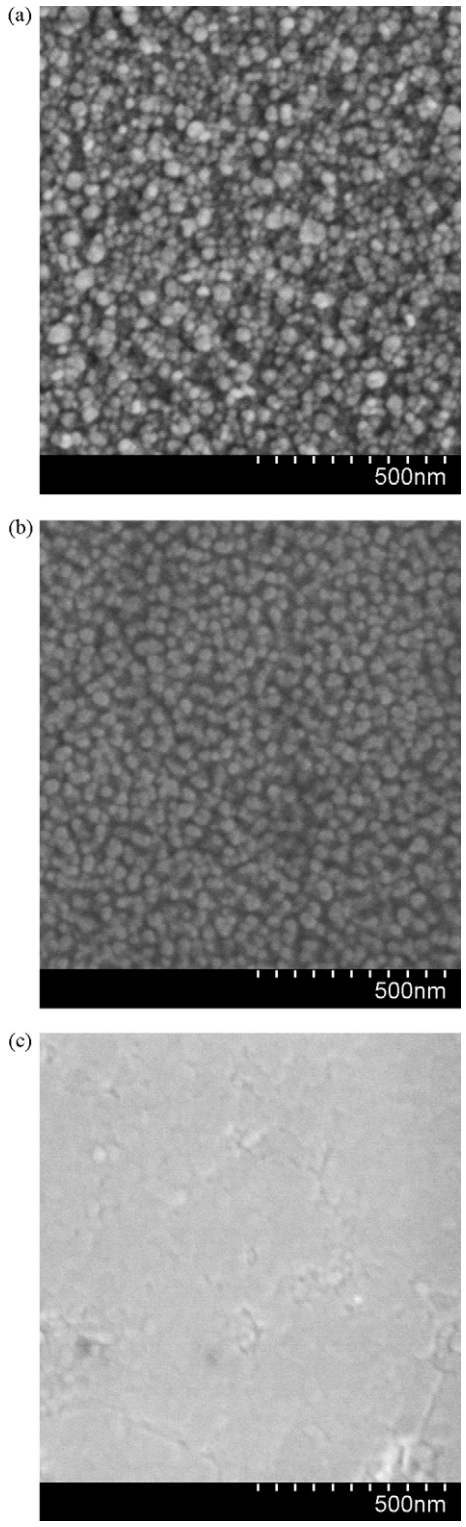

Fig. 2. SEM micrographs of the surface of $Ga_{2x}In_{2(1-x)}O_3$ films. Images (a), (b) and (c) correspond to $x = 0.1$, 0.5 and 0.9, respectively.

Fig. 5 shows the transmittance spectra of the $Ga_{2x}In_{2(1-x)}O_3$ samples with different Ga content as a function of wavelength in the range of 200–800 nm. Curves a, b, c, d and e correspond to $x = 0.1$, 0.3, 0.5, 0.7 and 0.9, respectively. Curves f is the transmittance spectrum of the ZrO_2 (1 0 0) substrate with a 0.5 mm thickness. The average transmittance of the samples in the visible wavelength range exceeds 78%, which is higher than the substrate of 77%. This result

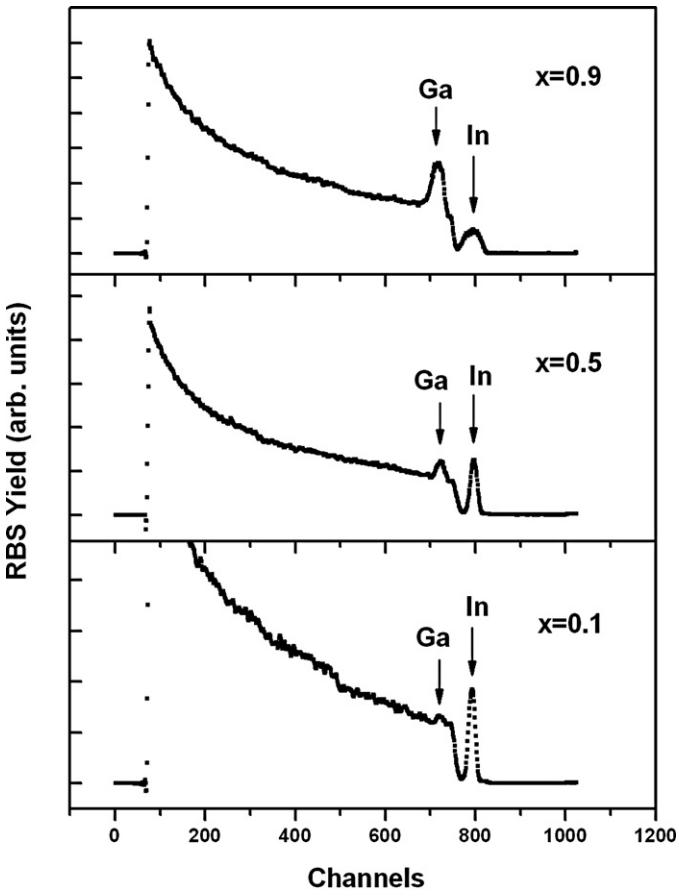

Fig. 3. RBS spectra of the $Ga_{2x}In_{2(1-x)}O_3$ films with experiment setting values $x = 0.1$, 0.5 and 0.9.

originates from the film thickness and the lower refractive index of the films compared with the substrate. The refractive index of Ga_2O_3 film is 1.80–1.91 [28], and the refractive index of In_2O_3 film is 1.92–2.00 [29]. The refractive index of this mixed oxide films can be estimated in the region of 1.80–2.00 as the TiO_2–SiO_2 mixed films [30,31]. The ZrO_2 substrate (commercially available) used in the experiment has a higher refractive index of about 2.14. The film thickness (89–162 nm) approximates a quarter of the wavelength of the visible wavelength range (380–780 nm). So the films could be considered as antireflective coatings in most of the visible wave-

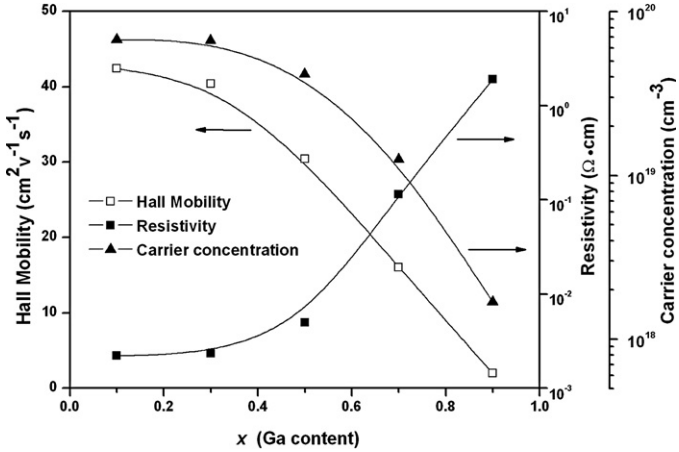

Fig. 4. The resistivity, Hall mobility and carrier concentration of the $Ga_{2x}In_{2(1-x)}O_3$ films as a function of Ga content.

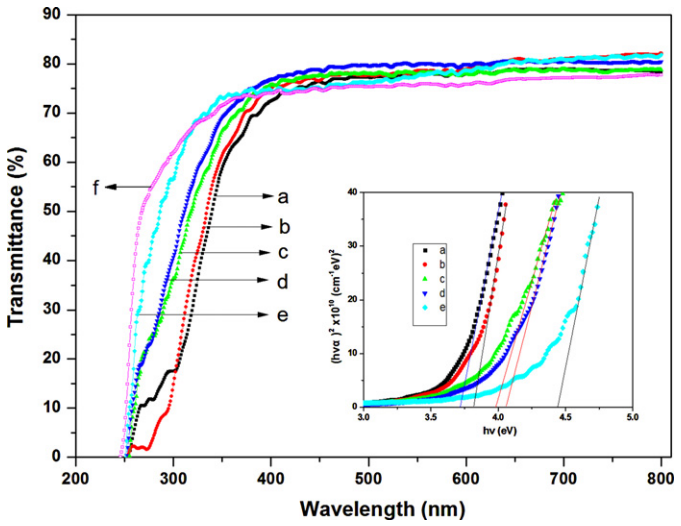

Fig. 5. The transmittance spectra of the $Ga_{2x}In_{2(1-x)}O_3$ samples: curves a, b, c, d, e and f correspond to $x = 0.1, 0.3, 0.5, 0.7, 0.9$ and the substrate, respectively. The plot of $(h\nu\alpha)^2$–hν is shown in the inset.

length range. As Ga content increases, the absorption edge of the films shifts to the shorter wavelength, which is attributed to the band gap of the films becomes wider. The spectra of a–d show a shoulder and go to zero at the same wavelength of about 255 nm, especially for the shape of curves a and b. The absorption edge of curves a and b is mainly determined by the bixbyite In_2O_3 phase, while the absorption edge of curves c and d is determined by the mixed phase. The shoulders of the spectra suggest the phase separation of Ga_2O_3 and In_2O_3 [21]. Also the shoulders of curves a and b which are obviously observed might be due to the low packing density Ga_2O_3 phase in the films. Curve e which has only a sharp absorption edge is mainly determined by the amorphous Ga_2O_3 phase. All the spectra of the $Ga_{2x}In_{2(1-x)}O_3$ samples go to zero at the same energy of about 4.86 eV, which is close to the band gap of Ga_2O_3 (4.9 eV), and this result is due to the existence of Ga_2O_3 phase more or less in the films.

The optical absorption coefficient (α) is given by the Beer–Lambert Law [Eq. (1)],

$$I = I_o e^{-ad} \tag{1}$$

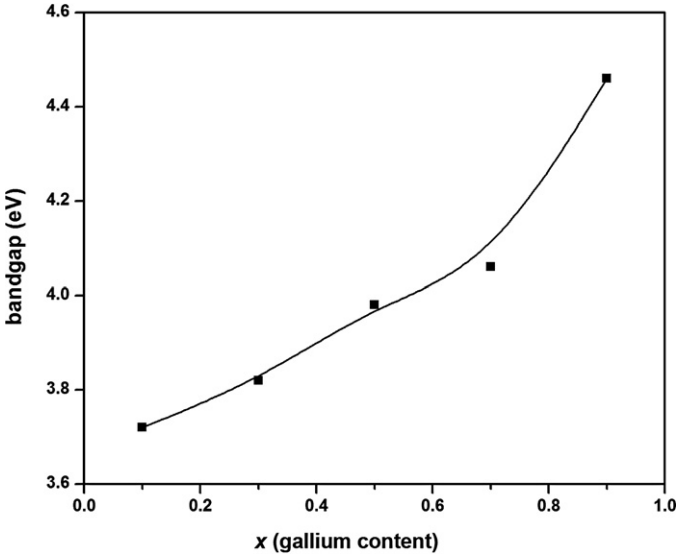

Fig. 6. The band gap of the $Ga_{2x}In_{2(1-x)}O_3$ films as a function of Ga content.

where I is the intensity of transmitted light, I_o is the intensity of incident light and d is the thickness of the film. For direct transition semiconductors, α and optical band gap (Eg) are related by Eq. (2) [32,33],

$$\alpha h\nu = A(h\nu - \mathrm{Eg})^{1/2} \tag{2}$$

where, h is the Planck's constant, ν is the frequency of the incident photon and A is a material dependent constant. Then the band gap of the films can be obtained by plotting $(h\nu\alpha)^2$ vs. $h\nu$ and extrapolating the straight-line portion of the plot to the energy axis. The plot of $(h\nu\alpha)^2$ as a function of $h\nu$ is shown in the inset of Fig. 5. Fig. 6 shows the band gap of the films as a function of Ga content. As x increases from 0.1 to 0.9, the band gap increases monotonously from 3.72 to 4.46 eV. These results imply that the band gap of the $Ga_{2x}In_{2(1-x)}O_3$ film can be tuned from 3.72 to 4.46 eV by controlling the Ga content in this semiconductor alloy suitably.

4. Conclusions

$Ga_{2x}In_{2(1-x)}O_3$ films with different Ga content have been deposited on ZrO_2 (1 0 0) substrates at 550 °C by MOCVD. The crystalline quality of the films decreased as Ga content increased. Corresponding to the Ga content increased from 0.1 to 0.9, the Hall mobility decreased from 42.40 to 1.96 $cm^2\ v^{-1}\ s^{-1}$ and the carrier concentration decreased from 6.70×10^{19} to $1.68 \times 10^{18}\ cm^{-3}$. In the mean time, the resistivity monotonously increased from 2.20×10^{-3} to 1.90 Ω cm. The average transmittance of the samples in the visible range exceeded 78% and the band gap can be tuned from 3.72 to 4.46 eV by controlling the composition of this semiconductor alloy. These results indicate that the $Ga_{2x}In_{2(1-x)}O_3$ film is a promising material which has high potential applications in the fields of quantum-well devices, short wavelength light emitting devices, UV photodetectors and so on.

Acknowledgement

This work is financially supported by the National Natural Science Foundation of China (Grant No. 50672054).

References

[1] D. Fritsch, H. Schmidt, M. Grundmann, Appl. Phys. Lett. 88 (2006) 134104.
[2] S. Han, D.Z. Shen, J.Y. Zhang, Y.M. Zhao, D.Y. Jiang, Z.G. Ju, D.X. Zhao, B. Yao, J. Alloys Compd. 485 (2009) 794–797.
[3] H. Tanaka, Sg. Fujita, Sz. Fujita, Appl. Phys. Lett. 86 (2005) 192911.
[4] R. Sharma, R.S. Mane, S.K. Min, S.H. Han, J. Alloys Compd. 479 (2009) 840–843.
[5] T. Oshima, N. Arai, N. Suzuki, S. Ohira, S. Fujita, Thin Solid Films 516 (2008) 5768–5771.
[6] A. Oprea, A. Gurlo, N. Barsan, U. Weimar, Sens. Actuators B 139 (2009) 322–328.
[7] C.H. Liang, G.W. Meng, Y. Lei, F. Phillipp, L. Zhang, Adv. Mater. 13 (2001) 1330–1333.
[8] D. Beena, K.J. Lethy, R. Vinodkumar, A.P. Detty, V.P. Mahadevan Pillai, V. Ganesan, J. Alloys Compd. 489 (2010) 215–223.
[9] W.H. Ho, C.F. Li, H.C. Liu, S.K. Yen, J. Power Sources 175 (2008) 897–902.
[10] M. Orita, H. Ohta, M. Hirano, H. Hosono, Appl. Phys. Lett. 77 (2000) 4166–4168.
[11] G. Sinha, D. Ganguli, S. Chaudhuri, J. Colloid Interf. Sci. 319 (2008) 123–129.
[12] X. Liu, G. Qiu, Y. Zhao, N. Zhang, R. Yi, J. Alloys Compd. 439 (2007) 275–278.
[13] Q. Xu, S. Zhang, Superlattices Microstruct. 44 (2008) 715–720.
[14] S. Ohira, T. Sugawara, K. Nakajima, T. Shishido, J. Alloys Compd. 402 (2005) 204–207.
[15] R. Hill, J. Phys. C: Solid State Phys. 7 (1974) 521–526.
[16] G. Patzke, M. Binnewies, Solid State Sci. 2 (2000) 689–699.
[17] H.J. Chun, Y.S. Choi, S.Y. Bae, H.C. Choi, J. Park, Appl. Phys. Lett. 85 (2004) 461–463.
[18] R.J. Cava, J.M. Phillips, J. Kwo, G.A. Thomas, R.B. van Dover, S.A. Carter, J.J. Krajewski, W.F. Peck Jr., J.H. Marshall, D.H. Rapkine, Appl. Phys. Lett. 64 (1994) 2071–2072.
[19] D.Y. Cho, J. Song, C.S. Hwang, W.S. Choi, T.W. Noh, J.Y. Kim, H.G. Lee, B.G. Park, S.Y. Cho, S.J. Oh, J.H. Jeong, J.K. Jeong, Y.G. Mo, Thin Solid Films 518 (2009) 1079–1081.
[20] K. Inoue, K. Tominaga, T. Tsuduki, M. Mikawa, T. Moriga, Vacuum 83 (2009) 552–556.
[21] T. Oshima, S. Fujita, Phys. Stat. Sol. C 5 (2008) 3113–3115.

[22] J.H. Lim, E.J. Yang, D.K. Hwang, J.H. Yang, J.Y. Oh, S.J. Park, Appl. Phys. Lett. 87 (2005) 042109.
[23] R.E. Presley, D. Hong, H.Q. Chiang, C.M. Hung, R.L. Hoffman, J.F. Wager, Solid State Electron. 50 (2006) 500–503.
[24] Y.G. Wang, S.P. Lau, H.W. Lee, S.F. Yu, B.K. Tay, X.H. Zhang, H.H. Hng, J. Appl. Phys. 94 (2003) 354–358.
[25] A. Bourlange, D.J. Payne, R.G. Palgrave, J.S. Foord, R.G. Egdell, R.M.J. Jacobs, A. Schertel, J.L. Hutchison, P.J. Dobson, Thin Solid Films 517 (2009) 4286–4294.
[26] H.W. Kim, N.H. Kim, J. Alloys Compd. 389 (2005) 177–181.
[27] W.K. Chu, J.W. Mayer, M.A. Nicolet, Backscattering Spectrometry, first ed., Academic Press, New York, 1978.
[28] M. Passlack, N.E.J. Hunt, E.F. Schubert, G.J. Zydzik, M. Hong, J.P. Mannaerts, R.L. Opila, R.J. Fischer, Appl. Phys. Lett. 64 (1994) 2715–2717.
[29] P. Prathap, Y.P.V. Subbaiah, M. Devika, K.T. Ramakrishna Reddy, Mater. Chem. Phys. 100 (2006) 375–379.
[30] S. Chao, W.H. Wang, M.Y. Hsu, L.C. Wang, J. Opt. Soc. Am. A 16 (1999) 1477–1483.
[31] S.K. Medda, S. De, G. De, J. Mater. Chem. 15 (2005) 3278–3284.
[32] X.T. Gao, I.E. Wachs, J. Phys. Chem. B 104 (2000) 1261–1268.
[33] R.K. Gupta, K. Ghosh, R. Patel, P.K. Kahol, J. Cryst. Growth 310 (2008) 4336–4339.